Computational Methods for Differential Equations
http://cmde.tabrizu.ac.ir
Vol. 5, No. 2, 2017, pp. 170-188

A wavelet method for stochastic Volterra integral equations and its application to general stock model

Saeed Vahdati
Department of Mathematics,
Khansar Faculty of Mathematics and Computer Science, Khansar, Iran.
E-mail: s.vahdati@khn.ui.ac.ir

Abstract In this article, we present a wavelet method for solving stochastic Volterra integral equations based on Haar wavelets. First, we approximate all functions involved in the problem by Haar Wavelets then, by substituting the obtained approximations in the problem, using the Itô integral formula and collocating at points then, the main problem converts to a system of linear or nonlinear equation which can be solved by some numerical methods like Newton's or Broyden's methods. The capability of the simulation of Brownian motion with Schauder functions which are the integration of Haar functions enables us to find some reasonable approximate solutions. Two test examples and the application of the presented method for the general stock model are considered to demonstrate the efficiency, high accuracy and the simplicity of the presented method.

Keywords. Haar Function, Schauder Function, Haar Wavelet, Itô Integral, Brownian Motion.
2010 Mathematics Subject Classification. 65T60, 60H20, 60H35, 60J65.

1. Introduction

Linear, nonlinear Volterra integral equations and integro-differential equations have an important role in theoretical physics and other disciplines. Several numerical approaches have been suggested for solving these equations, one can find an overview in the monograph. Beginning from 1991 onwards, some numerical methods based on wavelet theory has been applied for solving integral equations. A short investigation on these papers can be found in [12]. The solutions by these methods are often quite intricate and the merits of the wavelet method get lost, therefore, some researchers tried to find a simplified version of these methods. One way to do this, is to make use of the Haar wavelets, the most simple wavelets. An overview of the using of Haar wavelet method for solving linear integral equations related to a different and nonlinear Fredholm integral equations can be found in [12] and [13] respectively. Operational matrix of integration based on Haar wavelets and its application to analyse lumped and distributed-parameters dynamic systems established and formulated in [6]. For some other kind of wavelets such as Legendre multi-wavelets and their application one can refer to [1, 2, 8, 12, 13].

Received: 11 August 2016 ; Accepted: 14 December 2016.

Many problems in finance, mechanics, biology, medical, social sciences etc can be modeled by stochastic integral equations. The application of the stochastic integral equations for the modeling of such problems makes the study of these problems very useful and there is an increasing demand for studying the behavior of a number of sophisticated dynamical systems in physical, medical and social sciences, as well as in engineering and finance. The mentioned systems are usually dependent on a noise source, such as Gaussian white noise. For this reason, the modeling of such systems mostly requires the use of various stochastic functional equations. For stochastic differential equation case one can refer to [9, 10, 11, 14, 15, 16]. Some applications of stochastic Volterra and Volterra-Fredholm integral equations and stochastic integro-differential equations can be found in [7, 24, 25]. Finding an approximate solution for such problems by using a numerical method is so important because many cases of these problems cannot be solved analytically [7, 9, 10, 11, 14, 15, 16, 24, 25].

Haar wavelet operational matrix method is utilized for fractional order nonlinear oscillation equations by Saeed et. al [18]. They obtained the solutions of fractional order force-free and forced Duffing-Van der Pol oscillator and higher order fractional Duffing equation on large intervals. The combination of signal denoising technology and Hankel transforms algorithm which were both based on Haar wavelet decomposition is proposed in [23]. Zedan et. al [22] proposed a numerical solution based on Haar wavelet method for Fredholm integral equations and the system of Volterra integral equations.

Wavelet constitutes a family of functions constructed from dilation and translation of a single function called the mother wavelet. When the dilation parameter a and the translation parameter b vary continuously, we have the following family of continuous wavelets as [5],

$$\Psi_{a,b}(t) = |a|^{-1} \Psi\left(\frac{t-b}{a}\right), \ a, b \in \mathbb{R}, \ a \neq 0,$$

where Ψ is the mother wavelet.

Let $\alpha > 1$, $\beta > 0$ and l, and k are positive integers and restrict the parameters a and b to the discrete values as $a = \alpha^{-k}$, $b = l\beta\alpha^{-k}$, so the following discrete wavelets are obtained

$$\Psi_{l,k}(t) = |a|^{\frac{k}{2}} \Psi\left(\alpha^k t - l\beta\right),$$

which form a wavelet basis for $L^2(\mathbb{R})$. For the case, $\alpha = 2$ and $\beta = 1$ then $\Psi_{l,k}(t)$ forms an orthonormal basis [5].

2. Haar wavelet and function approximation

The Haar wavelet family is

$$\psi_n(s) = \begin{cases} 1, & \frac{k}{2^j} \leq s < \frac{2k+1}{2^{j+1}}, \\ -1, & \frac{2k+1}{2^{j+1}} \leq s < \frac{k+1}{2^j}, \\ 0, & elsewhere, \end{cases} \tag{2.1}$$

TABLE 1. The calculation of indices n, j, m and k for $J = 2$.

$J = 3,\ 2M = 2^{J+1} = 8$								
$n = 1 \cdots 2M$	1	2	3	4	5	6	7	8
$j = \lfloor \log_2(n-1) \rfloor$	-	0	1	1	2	2	2	2
$m = 2^j$	-	1	2	2	4	4	4	4
$k = n - m - 1$	-	0	0	1	0	1	2	3

the integer $m = 2^j$, $j = 0, 1, ..., J$ indicates the level of the wavelet; $k = 0, 1, ..., m-1$ is the translation parameter, the integer J determines the maximal level of resolution and the index n is calculated by the formula $n = m + k + 1$. The minimal value is $n = 2$ (then $m = 1$, $k = 0$)and the maximal value is $n = 2M$ where $M = 2^J$. The index $n = 1$ corresponds to the scaling function

$$\psi_1(s) = \begin{cases} 1, & 0 \le s < 1, \\ 0, & elsewhere. \end{cases} \tag{2.2}$$

It easy to see from what we have defined the indices through this section that for a fixed positive integer $n \ge 2$, we have $j = \lfloor \log_2(n-1) \rfloor$, $m = 2^j$ and $k = n - m - 1$. As an example, when $J = 3$ remaining indices are listed in Table 1.
The function $\psi_2(s)$ is called the mother wavelet, and all the other Haar Wavelets family except the scaling function are obtained from the mother wavelets by the operations of dilation and translation. This family of function are orthogonal to each other, so any function $f(s)$ which is square integrable in $(0, 1)$ can be expressed as an infinite sum of Haar Wavelets as follow

$$f(s) = \sum_{n=1}^{\infty} f_n \psi_n(s). \tag{2.3}$$

It is not difficult to see that the series (2.3) terminates at finite term if $f(s)$ is piecewise constant and the jumps are at points with a finite binary representation. In other cases, the truncation of the above series is given as an approximation of the function $f(s)$ for piecewise constant during each subinterval. The orthogonal property of Haar Wavelet family leads us to find the values of $f_n,\ n = 1, 2, \cdots$ as

$$\begin{aligned} f_1 &= \int_0^1 f(s)\psi_1(s)ds, \\ f_n &= 2^j \int_0^1 f(s)\psi_n(s)ds, n = 2 \cdots 2M,\ j = \lfloor \log_2(n-1) \rfloor. \end{aligned} \tag{2.4}$$

Imran Aziz [3] introduced a new algorithm to approximate the Haar wavelet coefficients. To do this, consider the following collocation points

$$s_p = \frac{p - 0.5}{2M},\ p = 1, 2, \cdots, 2M. \tag{2.5}$$

Let $f(s)$ be a square integrable function which has been approximated by Haar wavelets as follow

$$f(s) \simeq \hat{f}_{2M}(s) = \sum_{i=1}^{2M} \hat{f}_{i,2M}\psi_i(s), \tag{2.6}$$

substituting the collocation points (2.5) into (2.6) and supposing $f = \hat{f}_{2M}$ at the collocation points, we get the following linear system of equations

$$f(s_p) = \hat{f}_{2M}(s_p) = \sum_{i=1}^{2M} \hat{f}_{i,2M}\psi_i(s_p), \ (p = 1, 2, \cdots, 2M), \tag{2.7}$$

which is a $2M \times 2M$ linear system of equations. The following theorem is used to find the solution of this system for the unknown coefficients $\hat{f}_{i,2M}$. We will show that $\hat{f}_{i,2M}$, $i = 1, \cdots, 2M$ are the midpoint quadrature weights.

Theorem 2.1. *The solution of system (2.7) is given as follows*

$$\hat{f}_{1,2M} = \frac{1}{2M} \sum_{j=1}^{2M} f(s_j), \tag{2.8}$$

$$\begin{aligned} \hat{f}_{i,2M} &= \frac{1}{\rho_i} \left(\sum_{p=\alpha_i}^{\beta_i} f(s_p) - \sum_{p=\beta_i+1}^{\gamma_i} f(s_p) \right), \\ i &= 2, 3, \cdots, 2M, \end{aligned} \tag{2.9}$$

where

$$\begin{aligned} \alpha_i &= \rho_i(\sigma_i - 1) + 1, \\ \beta_i &= \rho_i(\sigma_i - 1) + \frac{\rho_i}{2}, \\ \gamma_i &= \rho_i\sigma_i, \\ \rho_i &= \frac{2M}{\tau_i}, \\ \sigma_i &= i - \tau_i, \\ \tau_i &= 2^{\lfloor \log_2(i-1) \rfloor}. \end{aligned}$$

Proof. See [3] and [21]. □

Now, consider a square integrable function $f(s,t)$ of two variables s and t. Using the Haar wavelet basis, this function can be approximated as follows

$$\hat{f}_{2M}(s,t) = \sum_{i=1}^{2M} \hat{f}_{i,2M}(t)\psi_i(s), \tag{2.10}$$

with a similar argument to the equation (2.6) and the collocation points given in (2.5), we have the following system of $2M \times 2M$ linear equations

$$f(s_p,t) = \sum_{i=1}^{2M} \hat{f}_{i,2M}(t)\psi_i(s_p), \ p = 1, 2, \cdots, 2M. \tag{2.11}$$

The following corollary renders an algorithm for finding the unknown coefficients $\hat{f}_{i,2M}(t)$.

Corollary 2.2. *The solution of the system (2.11) is given as follows*

$$\hat{f}_{1,2M}(t) = \frac{1}{2M}\sum_{j=1}^{2M} f(s_j,t), \tag{2.12}$$

$$\begin{aligned} \hat{f}_{i,2M}(t) &= \frac{1}{\rho_i}\left(\sum_{p=\alpha_i}^{\beta_i} f(s_p,t) - \sum_{p=\beta_i+1}^{\gamma_i} f(s_p,t)\right), \\ i &= 2,3,\cdots,2M, \end{aligned} \tag{2.13}$$

where $\tau_i, \sigma_i, \rho_i, \gamma_i, \beta_i$ and α_i are defined in theorem (2.1).

Proof. See [20]. □

Lemma 2.3. *Let $f \in C^2[0,1]$, $\|f''\|_\infty \leq \mathcal{M}$, $\{\hat{f}_{n,2M}\}_M$ be the sequence defined in (2.8) and (2.9) and f_n be the Haar wavelet coefficient defined in (2.4) then $\lim_{M\to\infty} \hat{f}_{n,2M} = f_n$, in particular $\left|\hat{f}_{1,2M} - f_1\right| \leq \frac{\mathcal{M}}{96M^2}$ and $\left|\hat{f}_{n,2M} - f_n\right| \leq \frac{\mathcal{M}}{192M^2}$, $n \geq 2$.*

Proof. For the case $n = 1$ we have

$$\begin{aligned} \left|\hat{f}_{1,2M} - f_1\right| &= \left|\frac{1}{2M}\sum_{j=1}^{2M} f(s_j) - \int_0^1 f(t)\psi_1(t)dt\right| \\ &= \left|\int_0^1 f(t)dt - \frac{1}{2M}\sum_{j=1}^{2M} f(s_j)\right| \leq \frac{\mathcal{M}}{96M^2}, \end{aligned} \tag{2.14}$$

the last inequality holds due to the error-bound composite midpoint rule of the numerical integration.

Now, let $n \geq 2$ be a positive integer number. Simply put, in the rest of the article we put $\epsilon_n = \frac{k}{2^j}$, $\zeta_n = \frac{2k+1}{2^{j+1}}$ and $\eta_n = \frac{k+1}{2^j}$, where j and k are the integer number regarding n as shown in Table 1.

$$\begin{aligned} \left|\hat{f}_{n,2M} - f_n\right| &= \\ &\left|\tfrac{1}{\rho_n}\left(\sum_{p=\alpha_n}^{\beta_n} f(s_p) - \sum_{p=\beta_n+1}^{\gamma_n} f(s_p)\right) - 2^j\int_0^1 f(t)\psi_n(t)dt\right| \\ &\leq \left|\tfrac{1}{\rho_n}\sum_{p=\alpha_n}^{\beta_n} f(s_p) - 2^j\int_{\epsilon_n}^{\zeta_n} f(t)dt\right| \\ &+ \left|\tfrac{1}{\rho_n}\sum_{p=\beta_n+1}^{\gamma_n} f(s_p) - 2^j\int_{\zeta_n}^{\eta_n} f(t)dt\right|, \end{aligned} \tag{2.15}$$

with some elementary calculations, we have

$$\begin{cases} \alpha_n = \frac{2Mk}{2^j} + 1, \\ \beta_n = \frac{2Mk}{2^j} + \frac{M}{2^j}, \\ \gamma_n = \frac{2Mk}{2^j} + \frac{2M}{2^j}, \\ \rho_n = \frac{2M}{2^j}, \end{cases} \tag{2.16}$$

and

$$\begin{cases} \beta_n - \alpha_n + 1 = \frac{M}{2^j}, \\ \gamma_n - (\beta_n + 1) + 1 = \frac{M}{2^j}, \\ s_p = \epsilon_n + \frac{1}{4M}, \ p = \alpha_n, \\ s_p = \zeta_n - \frac{1}{4M}, \ p = \beta_n, \\ s_p = \zeta_n + \frac{1}{4M}, \ p = \beta_n + 1, \\ s_p = \eta_n - \frac{1}{4M}, \ p = \gamma_n, \end{cases} \tag{2.17}$$

by using the equations (2.16), (2.17) and the composite midpoint rule, we obtain

$$\begin{aligned} \left| \frac{1}{\rho_n} \sum_{p=\alpha_n}^{\beta_n} f(s_p) - 2^j \int_{\epsilon_n}^{\zeta_n} f(t)dt \right| &\leq 2^j \frac{(\zeta_n - \epsilon_n)^3}{24 \left(\frac{M}{2^j}\right)^2} \\ &= \frac{\mathcal{M}}{192M^2}, \end{aligned} \tag{2.18}$$

and similarly

$$\begin{aligned} \left| \frac{1}{\rho_n} \sum_{p=\beta_n+1}^{\gamma_n} f(s_p) - 2^j \int_{\zeta_n}^{\eta_n} f(t)dt \right| &\leq 2^j \frac{(\eta_n - \zeta_n)^3}{24 \left(\frac{M}{2^j}\right)^2} \\ &= \frac{\mathcal{M}}{192M^2}. \end{aligned} \tag{2.19}$$

By considering equations (2.14), (2.18) and (2.19), we get

$$\lim_{M\to\infty} \hat{f}_{n,2M} = f_n.$$

□

Theorem 2.4. *Let $f \in C^2[0,1]$, $\|f''\|_\infty \leq \mathcal{M}$ then $\lim_{M\to\infty} \left\| f - \hat{f}_{2M} \right\|_2 = 0$.*

Proof. Haar wavelet family is dense in $L^2[0,1)$ which means

$$\lim_{M\to\infty}\left\|f-\sum_{n=1}^{2M}f_n\psi_n\right\|_2=0, \tag{2.20}$$

further

$$\begin{aligned}\left\|f-\hat{f}_{2M}\right\|_2 &\leq \left\|f-\sum_{n=1}^{2M}f_n\psi_n+\sum_{n=1}^{2M}f_n\psi_n-\hat{f}_{2M}\right\|_2\\ &\leq \left\|f-\sum_{n=1}^{2M}f_n\psi_n\right\|_2+\left\|\sum_{n=1}^{2M}f_n\psi_n-\sum_{n=1}^{2M}\hat{f}_{n,2M}\psi_n\right\|_2\\ &\leq \left\|f-\sum_{n=1}^{2M}f_n\psi_n\right\|_2+\left\|\sum_{n=1}^{2M}\left(f_n-\hat{f}_{n,2M}\right)\psi_n\right\|_2\\ &\leq \left\|f-\sum_{n=1}^{2M}f_n\psi_n\right\|_2+\frac{\mathcal{M}}{48M},\end{aligned} \tag{2.21}$$

by using equations (2.20) and (2.21), we can get the desire result. □

In the next theorem, we will extend the above idea for a bivariate function. Let $f(s,t)$ be a square integrable function, by using the Haar wavelet basis, we have

$$f(s,t)=\sum_{n=1}^{\infty}\sum_{k=1}^{\infty}\psi_n(s)f_{n,k}\psi_k(t),$$

where

$$\begin{aligned}f_{n,k} &= 2^{j_n+j_k}\int_0^1\int_0^1 f(s,t)\psi_n(s)\psi_k(t)dsdt,\\ j_n &= \lfloor\log_2(n-1)\rfloor,\\ j_k &= \lfloor\log_2(k-1)\rfloor.\end{aligned} \tag{2.22}$$

On the other hand, we can approximate this function in another way by equation (2.10)

$$f(s,t)\simeq\sum_{k=1}^{2M}\hat{f}_{n,2M}(t)\psi_n(s),$$

where $\hat{f}_{n,2M}(t), n=1,2,\cdots,2M$ are defined in equations (2.12) and (2.13). Each function $\hat{f}_{n,2M}(t)$ also can be approximated as follows

$$\hat{f}_{n,2M}(t)\simeq\sum_{k=1}^{2M}\hat{f}_{n,k,2M}\psi_k(t),$$

where the coefficients $\hat{f}_{n,k,2M}$ are calculated by equations (2.8) and (2.9), so

$$f(s,t) \simeq \sum_{k=1}^{2M}\sum_{k=1}^{2M} \psi_n(s)\hat{f}_{n,k,2M}\psi_k(t),$$

under some assumptions and the following collocation points, we will show

$$\lim_{M\to\infty} \hat{f}_{n,k,2M} = f_{n,k},$$

$$t_q = \frac{q-0.5}{2M},\ q = 1,2,\cdots,2M. \tag{2.23}$$

Lemma 2.5. *Let* $\Omega = [0,1]^2$, $f \in C^2(\Omega)$, $I(f) := \int_0^1\int_0^1 f(s,t)dsdt$ *and* $Q_{2M}(f) := \frac{1}{4M^2}\sum_{n=1}^{2M}\sum_{k=1}^{2M} f(s_k,t_n)$ *where* s_k *and* t_k *are defined in (2.5) and (2.23), then*

$$|I(f) - Q_{2M}(f)| \le \frac{1}{96M^2}\left(\max_{(s,t)\in\Omega}\left|\frac{\partial^2 f}{\partial s^2}\right| + \max_{(s,t)\in\Omega}\left|\frac{\partial^2 f}{\partial t^2}\ |\right)\right.\!.$$

Proof. In a general case, let $\Omega = [a,b]\times[c,d]$ and $f(s,t) : \Omega \longrightarrow \mathbb{R}$ be a square integrable function. Suppose w_j and s_j, $j = 1,2,\cdots,m$ are the weights and nodes regarding one dimension numerical integral in s direction and w_i' and t_i, $i = 1,2,\cdots,n$ are weights and nodes regarding one dimension numerical integral in t direction. Let $F(s) = \int_c^d f(s,t)dt$, we have

$$\begin{aligned}
I(f) &:= \int_a^b\int_c^d f(s,t)dtds = \int_a^b F(s)ds \\
&= \sum_{j=1}^{m} F(s_j)w_j + E_s(F(s)) \\
&= \sum_{j=1}^{m}\left[\sum_{i=1}^{n} f(s_j,t_i)w_i' + E_t(f(s_j,t))\right] + E_s(F(s)) \\
&= \sum_{j=1}^{m}\sum_{i=1}^{n} f(s_j,t_i)w_i'w_j + \sum_{j=1}^{m} w_j E_t(f(s_j,t)) + E_s(F(s)) \\
&= Q_{m,n}(f) + E_{m,n}(f),
\end{aligned}$$

where, E_s and E_t are the errors of one dimension numerical integrations in direction s and t respectively and also

$$Q_{m,n}(f) := \sum_{j=1}^{m}\sum_{i=1}^{n} f(s_j,t_i)w_i'w_j,$$

$$E_{m,n}(f) := \sum_{j=1}^{m} w_j E_t(f(s_j,t)) + E_s(F(s)),$$

are the double numerical integration formula and the error terms. Suppose that the one dimension numerical integration, we have

$$|E_t(f(.,t))| \leq \bar{E}_t,\ |E_s(F(s))| \leq \bar{E}_s,$$

so

$$|I(f) - Q_{m,n}(f)| \leq W\bar{E}_t + \bar{E}_s, \tag{2.24}$$

where $W = \sum_{j=1}^{m} |w_j|$.

Now, in our special case, we use the midpoint rule ($Q_{2M}(f) = Q_{n,m}(f)$) where $a = c = 0, b = d = 1$, $m = n = 2M$, $w_j = w'_i = \frac{1}{2M}$, $h_s = h_t = \frac{1}{2M}$ where h_s and h_t are the distance between two subsequent points in direction s and t respectively. Using the assumption $f \in C^2_\Omega$, it is clear that

$$\bar{E}_s = \frac{1}{96M^2} \max_{(s,t)\in\Omega} \left|\frac{\partial^2 f}{\partial s^2}\right|,$$

$$\bar{E}_t = \frac{1}{96M^2} \max_{(s,t)\in\Omega} \left|\frac{\partial^2 f}{\partial t^2}\right|.$$

and $W = \sum_{j=1}^{m} |w_j| = 1$. Substituting the obtained results in (2.24) will complete the proof. □

Theorem 2.6. *Under the above assumptions, including the assumption that $f(s,t) \in C^2_\Omega$, where $\Omega = [0,1]^2$. Suppose $\max_{(s,t)\in\Omega} |\frac{\partial^2 f}{\partial s^2}| \leq \mathcal{M}_1$, $\max_{(s,t)\in\Omega} |\frac{\partial^2 f}{\partial t^2}| \leq \mathcal{M}_2$, then for each $k, n = 1, 2, \cdots, 2M$ we have $\lim_{M\to\infty} \hat{f}_{n,k,2M} = f_{n,k}$, in particular*

$$|\hat{f}_{n,k,2M} - f_{n,k}| \leq \frac{1}{96M^2}(\mathcal{M}_1 + \mathcal{M}_2).$$

Proof. It is clear to see

$$\begin{aligned} \hat{f}_{1,1,2M} &= \frac{1}{2M}\sum_{j=1}^{2M} \hat{f}_{1,2M}(t_j) = \frac{1}{4M^2}\sum_{j=1}^{2M}\sum_{i=1}^{2M} f(s_i,t_j) = Q_{2M}(f) \\ &= Q_{2M}(f\psi_1) = Q_{2M}(f\psi_1\psi_1), \end{aligned} \tag{2.25}$$

$$\begin{aligned} \underset{k=2,3,\cdots,2M}{\hat{f}_{1,k,2M}} &= \frac{1}{\rho_k}\left(\sum_{p=\alpha_k}^{\beta_k} \hat{f}_{1,2M}(t_p) - \sum_{p=\beta_k+1}^{\gamma_k} \hat{f}_{1,2M}(t_p)\right) \\ &= \frac{1}{2M\rho_k}\sum_{n=1}^{2M}\left(\sum_{p=\alpha_k}^{\beta_k} f(s_n,t_p) - \sum_{p=\beta_k+1}^{\gamma_k} f(s_n,t_p)\right) \\ &= 2^{j_k} Q_{2M}(f\psi_k) = 2^{j_k} Q_{2M}(f\psi_k\psi_1). \end{aligned} \tag{2.26}$$

Similarly, we have

$$\underset{n=2,3,\cdots,2M}{\hat{f}_{n,1,2M}} = 2^{j_n} Q_{2M}(f\psi_n) = 2^{j_n} Q_{2M}(f\psi_1\psi_n), \tag{2.27}$$

and

$$\underset{n,k=2,3,\cdots,2M}{\hat{f}_{n,k,2M}} = 2^{j_n+j_k} Q_{2M}(f\psi_n\psi_k). \tag{2.28}$$

By using equation (2.22), equations (2.25)-(2.28) and the lemma (2.5), we have

$$\lim_{M\to\infty} \hat{f}_{n,k,2M} = f_{n,k},\ n,k = 1,2,\cdots,2M,$$

and

$$|\hat{f}_{n,k,2M} - f_{n,k}| \le \frac{1}{96M^2}(\mathcal{M}_1 + \mathcal{M}_2).$$

□

Corollary 2.7. *With the same argument discussed in (2.4), let* $\Omega = [0,1]^2$, $f(s,t) \in C^2_\Omega$, $\max\limits_{(s,t)\in\Omega} |\frac{\partial^2 f}{\partial s^2}| \le \mathcal{M}_1$, $\max\limits_{(s,t)\in\Omega} |\frac{\partial^2 k}{\partial t^2}| \le \mathcal{M}_2$ *and* $\hat{f}_{2M}(s,t) = \sum\limits_{k=1}^{2M}\sum\limits_{k=1}^{2M} \psi_n(s)\hat{f}_{n,k,2M}\psi_k(t)$ *then* $\lim\limits_{M\to\infty} \left\| f - \hat{f}_{2M} \right\|_2 = 0.$

3. Simulation of Brownian motion via series representations

Definition 3.1. Let $(\Omega, \mathcal{F}, \mathbb{P})$ be a probability space and let $\{\mathcal{F}_t\}$ be a filtration, $B(t) = B_t = B_t(\omega)$ is a one-dimensional Brownian motion with respect to $\{\mathcal{F}_t\}$ and the probability measure $\mathbb{P}$, started at 0, if [4]

(1) B_t is $\mathcal{F}_t$ measurable for each $t \ge 0$.
(2) $B_0 = 0$, a.s.
(3) $B_t - B_s$ is a normal random variable with mean 0 and variance $t-s$ whenever $s < t$.
(4) $B_t - B_s$ is independent of $\mathcal{F}_s$ whenever $s < t$.
(5) B_t has continuous paths.

Since the Brownian sample paths are continuous functions, they can be expanded in a Fourier series. However, the paths are random functions: for different ω different functions are obtained. This means that the coefficients of this Fourier series are random variables, and since the process is Gaussian, they must be Gaussian as well. The representation of Brownian motion on the interval $[0, 2\pi]$ is called Paley-Wiener representation, which is formulated as follows [17]

$$\begin{aligned} B_t(\omega) &= Z_0(\omega)\frac{t}{\sqrt{2\pi}} + \frac{2}{\sqrt{\pi}}\sum_{n=1}^{\infty} Z_n(\omega)\frac{\sin(\frac{nt}{2})}{n}, \\ t &\in [0, 2\pi], \end{aligned}$$

where $(Z_n, n \ge 0)$ is a sequence of iid (independent and identically distributed) $N(0,1)$ random variables.

Another such well-known representation is due to Lévy representation, since the sine functions are replaced by certain polygonal functions (the Schauder function). Let's define the Haar functions H_n on $[0,1]$ as follows

$$H_1(t) = 1,$$

$$H_{2^{m+1}}(t) = \begin{cases} 2^{\frac{m}{2}}, & if \quad t \in \left[1 - \frac{2}{2^{m+1}}, 1 - \frac{1}{2^{m+1}}\right), \\ -2^{\frac{m}{2}}, & if \quad t \in \left[1 - \frac{1}{2^{m+1}}, 1\right), \\ 0, & elsewhere, \end{cases}$$

$$H_{2^m+k}(t) = \begin{cases} 2^{\frac{m}{2}}, & if \quad t \in \left[\frac{k-1}{2^m}, \frac{2k-1}{2^{m+1}}\right), \\ -2^{\frac{m}{2}}, & if \quad t \in \left[\frac{2k-1}{2^{m+1}}, \frac{k}{2^m}\right), \\ 0, & elsewhere, \end{cases}$$

$$k = 1, \ldots, 2^m - 1; \ m = 0, 1, \ldots.$$

From these functions, define the system of the Schauder functions on $[0,1]$ by integrating the Haar functions

$$\widetilde{H}_n(t) = \int_0^t H_n(s)ds, \ n = 1, 2, \ldots.$$

Figure 3 shows the graphs of H_n and $\widetilde{H}_n$ for the first n. A series representation for

FIGURE 1. The graphs of H_n and $\widetilde{H}_n$ for the first n.

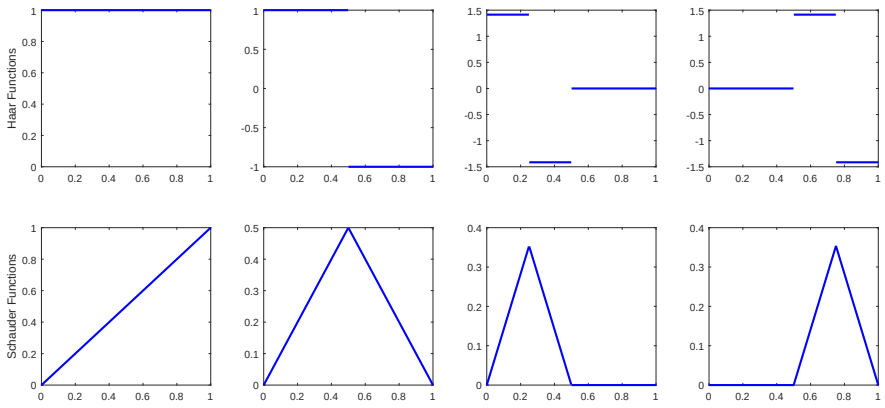

Brownian sample path on $[0,1]$ is then given by

$$B_t(\omega) = \sum_{n=1}^{\infty} Z_n(\omega)\widetilde{H}_n(t) \; t \in [0,1], \tag{3.1}$$

where the convergence of this series is uniform for $t \in [0,1]$ and $Z_n(\omega)$s are realizations of an iid $N(0,1)$ sequence (Z_n). Haar wavelet approximation of the involved functions in the problem, simulation of the Brownian motion by Haar functions and the similarities between the Haar wavelet family and Haar functions enable us to reduce the computational costs in solution procedure.

4. Stochastic integration operational matrix

In this section, we have applied the Itô integral for functions $\psi_n(s)$ as follows

$$\int_0^t \psi_n(s)dB(s) = \begin{cases} 0, \\ B(t) - B(\frac{k}{2^j}), \\ 2B(\frac{2k+1}{2^j}) - B(\frac{k}{2^j}) - B(t), \\ 2B(\frac{2k+1}{2^{j+1}}) - B(\frac{k}{2^j}) - B(\frac{k+1}{2^j}), \end{cases} \tag{4.1}$$

for

$$0 \le t < \frac{k}{2^j},$$

$$\frac{k}{2^j} \le t < \frac{2k+1}{2^{j+1}},$$

$$\frac{2k+1}{2^{j+1}} \le t < \frac{k+1}{2^j},$$

$$\frac{k+1}{2^j} \le t < 1,$$

respectively.
By substituting $t_q = \frac{q-0.5}{2M}$, $q = 1, 2, \cdots, 2M$ in (4.1) we have

$$\begin{aligned} \psi_n^B(t_q) &= \int_0^{t_q} \psi_n(s)dB(s) \\ &= \begin{cases} 0, & 0 \le t_q < \frac{k}{2^j}, \\ B(t_q) - B(\frac{k}{2^j}), & \frac{k}{2^j} \le t_q < \frac{2k+1}{2^{j+1}}, \\ 2B(\frac{2k+1}{2^j}) - B(\frac{k}{2^j}) - B(t_q), & \frac{2k+1}{2^{j+1}} \le t_q < \frac{k+1}{2^j}, \\ 2B(\frac{2k+1}{2^{j+1}}) - B(\frac{k}{2^j}) - B(\frac{k+1}{2^j}), & \frac{k+1}{2^j} \le t_q < 1, \end{cases} \end{aligned} \tag{4.2}$$

where it can be written in a matrix form, so called stochastic integration operational matrix

$$P^B_{Haar} = \left[\psi^B_i(t_q)\right]_{2M\times 2M},\ i,q = 1,2,\cdots,2M.$$

5. Solution procedure

In this section, we will describe the numerical method for stochastic Volterra integral equations. We consider the following stochastic Volterra integral equation

$$X(t) = f(t) + \int_0^t k_1(s,t,X(s))ds + \int_0^t k_2(s,t,X(s))dB(s),\ t\in[0,1), \tag{5.1}$$

where X, f, k_1 and k_2 are the stochastic processes defined on the probability space $(\Omega,\mathbb{F},\mathbb{P})$, and X is unknown. Also, $B(t)$ is a Brownian motion and $\int_0^t k_2(s,t,X(s))dB(s)$ is the Itô integral. Using equation (2.11), we approximate the functions $k_1(s,t,X(s))$ and $k_2(s,t,X(s))$ as follow

$$k_l(s,t,X(s)) = \sum_{i=1}^{2M}\hat{k}_{l,i}(t)\psi_i(s),\ l=1,2,$$

where

$$\hat{k}_{l,1}(t) = \frac{1}{2M}\sum_{j=1}^{2M}k_l(s_j,t,X(s_j)),\ l=1,2, \tag{5.2}$$

and

$$\begin{aligned}\hat{k}_{l,i}(t) &= \frac{1}{\rho_i}\left(\sum_{p=\alpha_i}^{\beta_i}k_l(s_p,t,X(s_p)) - \sum_{p=\beta_i+1}^{\gamma_i}k_l(s_p,t,X(s_p))\right)\\ i &= 2,3,\cdots,2M,\ l=1,2,\end{aligned} \tag{5.3}$$

by substituting the above approximations in equation (5.1), we obtain the following equation

$$X(t) = f(t) + \int_0^t \sum_{i=1}^{2M}\hat{k}_{1,i}(t)\psi_i(s)ds + \int_0^t \sum_{i=1}^{2M}\hat{k}_{2,i}(t)\psi_i(s)dB(s),\ t\in[0,1).$$

After simplifying and substituting the collocation points (2.23), we have

$$\begin{aligned} X(t_q) &= f(t_q) + \frac{1}{2M}\sum_{p=1}^{2M} k_1(s_p, t_q, X(s_p))\psi_1(t_q) \\ &+ \frac{1}{2M}\sum_{p=1}^{2M} k_2(s_p, t_q, X(s_p))\psi_1^B(t_q) \\ &+ \sum_{i=2}^{2M}\frac{1}{\rho_i}\left(\sum_{p=\alpha_i}^{\beta_i} k_1(s_p, t_q, X(s_p))\right. \\ &- \left.\sum_{p=\beta_i+1}^{\gamma_i} k_1(s_p, t, X(s_p))\right)\psi_i(t_q) \\ &+ \sum_{i=2}^{2M}\frac{1}{\rho_i}\left(\sum_{p=\alpha_i}^{\beta_i} k_2(s_p, t_q, X(s_p))\right. \\ &- \left.\sum_{p=\beta_i+1}^{\gamma_i} k_2(s_p, t, X(s_p))\right)\psi_i^B(t_q). \end{aligned} \tag{5.4}$$

Having Solved the above system of equations and used the equations (2.6)-(2.9), we can find the Haar wavelet approximation for the stochastic process $X(t)$ as follows

$$X(s) \simeq \hat{X}_{2M} = \sum_{i=1}^{2M} \hat{X}_{i,2M}\psi_i(s). \tag{5.5}$$

6. Numerical results

In order to demonstrate the method presented in the previous section, the following examples are considered.

Example 1. Consider the following linear stochastic Volterra integral equation,

$$X(t) = 1 + \int_0^t s^2 X(s)ds + \int_0^t sX(s)dB(s), \ \ s,t \in [0,1). \tag{6.1}$$

with the exact solution $X(t) = e^{\frac{t^3}{6}+\int_0^t sdB(s)}$ where $X(t)$ is an unknown stochastic process defined on the probability space $(\Omega, z, \mathbb{P})$, and $B(t)$ is a Brownian motion process.The curves in Figure 1 represents a trajectory of the approximate solution computed by the presented method with a trajectory of exact solution.

Example 2. Consider the following linear stochastic Volterra integral equation,

$$X(t) = \frac{1}{12} + \int_0^t \cos(s)X(s)ds + \int_0^t \sin(s)X(s)dB(s), \ \ s,t \in [0,1), \tag{6.2}$$

FIGURE 2. Simulation of Brownian motion are shown in graphs (a) with $J = 6$ and (c) with $J = 7$. Graphs (b) and (d) show the proposed analytical approximate and exact solutions of equation (6.1) corresponding to the simulation of Brownian motion shown in (b) and (d) respectively.

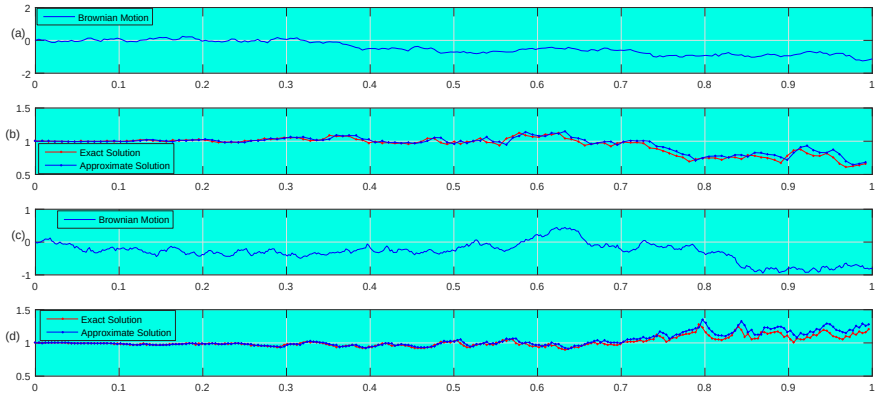

with the exact solution $X(t) = \frac{1}{12}e^{\frac{-t}{4}+\sin(t)+\frac{\sin(2t)}{8}+\int_0^t \sin(s)dB(s)}$ where $X(t)$ is an unknown stochastic process defined on the probability space (Ω, z, P), and $B(t)$ is a Brownian motion process.The curves in Figure 2 represents a trajectory of the approximate solution computed by the presented method with a trajectory of exact solution.

6.1. **Application to general stock model.** The market consists of a riskless cash bond, $\{A(t)\}_{t\geq 0}$, and a single risky asset with price process $\{S(t)\}_{t\geq 0}$ governed by

$$\begin{cases} dA_t = r_t A_t d_t, \ A_0 = 1, \\ dS_t = \mu_t S_t d_t + \sigma_t S_t dB_t, \end{cases} \tag{6.3}$$

where $\{W(t)\}_{t\geq 0}$ is a $\mathbb{P}$-Brownian motion generating the filtration $\{\mathcal{F}\}_{t\geq 0}$ and $\{r(t)\}_{t\geq 0}$, $\{\mu(t)\}_{t\geq 0}$ and $\{\sigma(t)\}_{t\geq 0}$ are $\{\mathcal{F}\}_{t\geq 0}$-adapted processes. Evidently, a solution to these equations should take the form

$$\begin{cases} A_t = exp\left(\int_0^t r_u du\right), \\ S_t = S_0 exp\left(\int_0^t \left(\mu_u - \frac{1}{2}\sigma_u^2\right) du + \int_0^t \sigma_u dB_u\right). \end{cases} \tag{6.4}$$

FIGURE 3. Simulation of Brownian motion are shown in graphs (a) with $J = 6$ and (c) with $J = 7$. Graphs (b) and (d) show the proposed analytical approximate and exact solutions of equation (6.2) corresponding to the simulation of Brownian motion shown in (b) and (d) respectively.

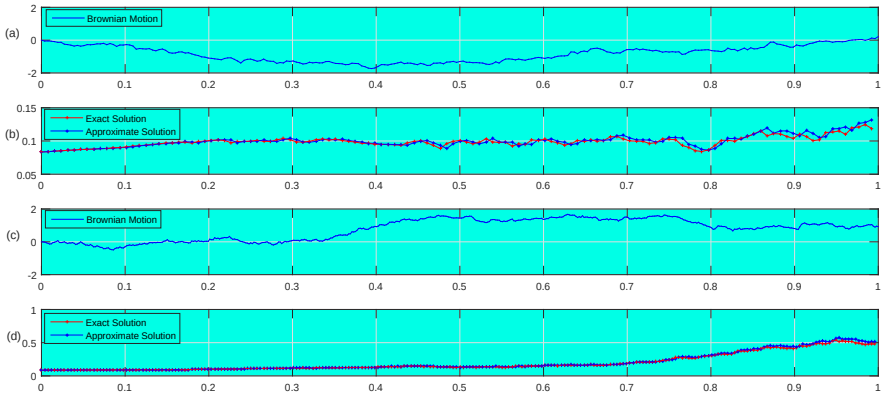

For example, consider the following general stock model,

$$\begin{cases} dA_u = \sin(u)A_u du, \ B_0 = 1, \ u \in [0,1), \\ S_t = \dfrac{1}{10} + \displaystyle\int_0^t \ln(1+u)S_u du + \int_0^t uS_u dB_u, \\ u, t \in [0,1), \end{cases} \tag{6.5}$$

with the exact solution $A_t = e^{1-\cos(t)}$ and $S_t = \frac{1}{10} e^{(1+t)\ln(1+t) - t - \frac{t^3}{6} + \int_0^t u dB_u}$, for $0 \le t < 1$. Figure 4 shows two trajectory of the analytical approximate solution computed by the presented method with the trajectory of the exact solutions for levels $J = 6$ and $J = 7$.

Theorem 6.1. *Let W_t, $t \ge 0$ be a Brownian motion, and let $\Delta(t)$ be a nonrandom function of time. Define $I(t) = \int_0^t \Delta(u) dB_u$. For $t \ge 0$, the random variable $I(t)$ is normally distributed with expected value zero and variance $\int_0^t \Delta^2(u) du$.*

Proof. See [19]. □

Corollary 6.2. *Theorem (6.1) implies that the random variables $\ln X(t)$ in examples (6.1) and (6.2) and $\ln S_t$ in example (6.5) are normally distributed. Therefore, confidence intervals for these random variables and thereafter for $X(t)$ and S_t can be obtained. As an special case, we have*

$$\ln S_t \sim \mathcal{N}\left(\ln \frac{1}{10} + (1+t)\ln(1+t) - t - \frac{t^3}{6}, \frac{t^2}{2} \right).$$

FIGURE 4. Simulation of Brownian motion are shown in graphs (a) with $J = 6$ and (c) with $J = 7$. Graphs (b) and (d) show the proposed analytical approximate and exact solutions of equation (6.5) corresponding to the simulation of Brownian motion shown in (b) and (d) respectively.

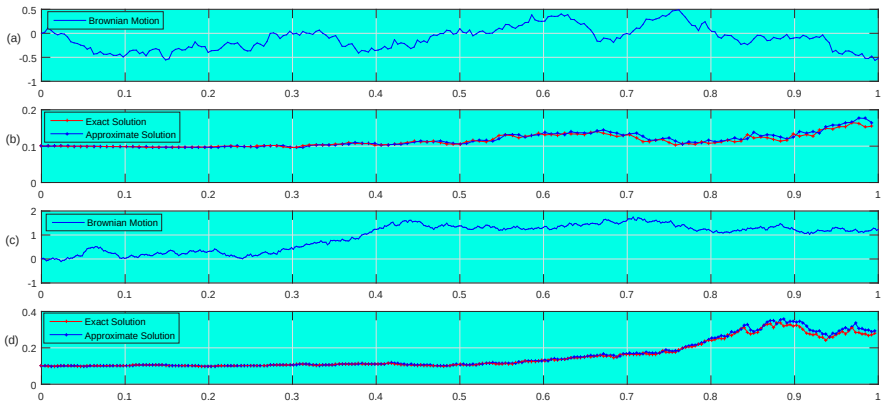

Figure 5 shows a 95% confidence region for the stock price process, in Figure 5-(a) 100 sample paths for the exact solution $S_t = \frac{1}{10}e^{(1+t)\ln(1+t)-t-\frac{t^3}{6}+\int_0^t udB_u}$ with the upper and lower limits corresponding to the 95% confidence region is shown where, Figure 5-(b) shows the approximate sample paths corresponding to 100 sample paths of the exact solution and the 95% confidence region.

7. Conclusion

Mail goal of the presented work has been to construct an approximation to the solution of stochastic Volterra integral equations. In the above discussion, the collocation points with Haar wavelets, which have the property of orthogonality, is employed to achieve this goal. Using the new method for finding the Haar wavelet coefficients enables us to reduce the computation costs. There is a good agreement between obtained results and exact values that demonstrate the validity of the present method for this type of problems and gives the method a wider applicability. The method also applied to general stock model and the obtained results showed the ability and the accuracy of the method.

Acknowledgment

The author was partially supported by a grant from Khansar Faculty of Mathematics and Computer Science (Khansar-CMC-005).

FIGURE 5. The 95% confidence region for the general stock model; Figure (a) shows the sample paths obtained from the exact solution where Figure (b) shows the sample paths obtained from the proposed method.

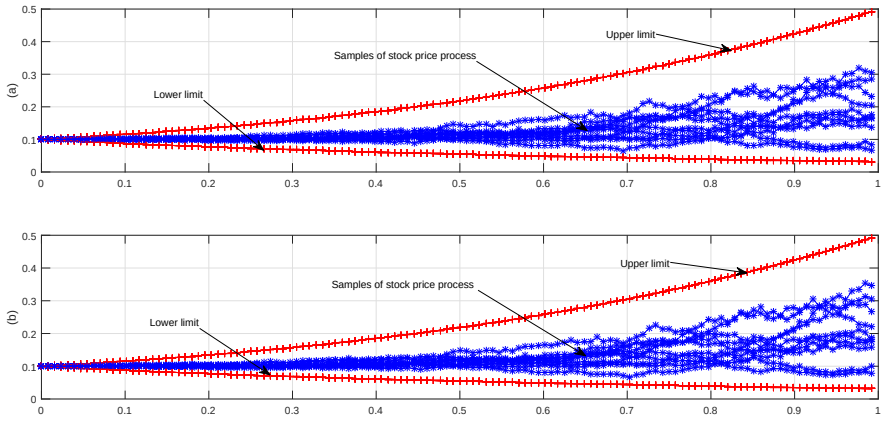

REFERENCES

[1] Z. Abbas, S. Vahdati, K. A. Atan, and N. M. A. N. Long, *Legendre multi-wavelets direct method for linear integro-differential equations*, Appl. Math. Sci., *3(14)* (2009), 693–700.

[2] Z. Abbas, S. Vahdati, and M. Ghasemi, *Legendre multi-wavelets direct method for solving fredholm integral equations of the second kind*, Aust. J. Basic Appl. Sci., *4(9)* (2010), 4193–4199.

[3] I. Aziz and Siraj-ul-Islam, *New algorithms for the numerical solution of nonlinear fredholm and volterra integral equations using Haar wavelets*, J. Comput. Appl. Math., *239* (2013), 333–345.

[4] R. F. Bass, *Stochastic Processes*, Cambridge University Press, 2011.

[5] A. Boggess and F. J. Narcowich, *A First Course in Wavelets with Fourier Analysis*, Prentice Hall, 2001.

[6] C. Chen and C. Hsiao, *Haar wavelet method for solving lumped and distributed-parameter systems*, IEE Proc. Control Theory Appl., *144(1)* (1997), 87–94.

[7] S. Jankovic and D. Ilic, *One linear analytic approximation for stochastic integro-differential equations*, Acta, Math. Sci., *30* (2010), 1073–1085.

[8] Y. Khan, M. Ghasemi, S. Vahdati, and M. Fardi, *Legendre multi-wavelets to solve oscillating magnetic fields integro-differential equations*, U.P.B. Sci. Bull., Series A, *76(1)* (2014), 51–58.

[9] M. Khodabin, K. Maleknejad, M. Rostami, and M. Nouri, *Numerical solution of stochastic differential equations by second order runge-kutta methods*, Math.

Comput. Model., *53(9)* (2011), 1910–1920.
[10] M. Khodabin, K. Maleknejad, M. Rostami, and M. Nouri, *Interpolation solution in generalized stochastic exponential population growth model*, Appl. Math. Model., *36(3)* (2012), 1023–1033.
[11] M. Khodabin, K. Maleknejad, M. Rostami, and M. Nouri, *Numerical approach for solving stochastic volterra-fredholm integral equations by stochastic operational matrix*, Comput. Math. Appl., *64(6)* (2012), 1903–1913.
[12] U. Lepik and E. Tamme. *Application of the Haar wavelets for solution of linear integral equations*, Dyn. Syst. Appl, Proc., (July, Antalya, Turkey), (2004), 494–507.
[13] U .LepikandE.Tamme.*Solution of nonlinear fredholm integral equations via the haar wavelet method*, Proc. Est. Acad. Scie. Phy. Math., (2017), 17–27.
[14] K. Maleknejad, M. Khodabin, and M. Rostami. *A numerical method for solving m-dimensional stochastic ito-volterra integral equations by sto- chastic operational matrix*, Comput. Math. Appl., *63(1)* (2012), 133–143.
[15] K. Maleknejad, M. Khodabin, and M. Rostami. *Numerical solution of stochastic volterra integral equations by a stochastic operational matrix based on block pulse functions*, Math. Compt. Model., *55(3)* (2012), 791–800.
[16] K. Maleknejad and F. Mirzaee. *Numerical solution of stochastic linear heat conduction problem by using new algorithms*, Appl. Math. Comput., *163(1)* (2005), 97–106.
[17] T. Mikosch. *Elementary Stochastic Calculus with Finance in view*, World Scientific, 1998.
[18] U. Saeed and M. ur Rehman. *Haar wavelet operational matrix method for fractional oscillation equations*, Int. J. of Math. Math. Sci., *2014* (2014).
[19] E. Shreve Steven. *Stochastic Calculus for Finance II: Continuous-Time Models*, Springer, 2004.
[20] Siraj-ul-Islam, Imran Aziz, A. S. Al–Fhaid, *An improved method based on Haar wavelets for numerical solution of nonlinear integral and integro- differential equations of first and higher orders*, J. Comput. Appl. Math., *260* (2014), 449–469.
[21] Siraj-ul-Islam, I. Aziz, Fazal Haq, *A comparative study of numerical integration based on Haar wavelets and hybrid functions*, Comput. Math. Appl., *59(6)* (2010), 2026–2036.
[22] H. A. Zedan and E. Alaidarous, *Haar wavelet method for the system of integral equations*, Abstr. Appl. Anal., *2014* (2014).
[23] H. Zhang, C. Zhu, X. Su, and X. Nie, *A stable hankel transforms algorithm based on Haar wavelet decomposition for noisy data*, Math. Prob. Eng., *2015* (2015).
[24] X. Zhang, *Euler schemes and large deviations for stochastic volterra equations with singular kernels*, J. Differ. Equ., *44* (2008), 2226– 2250.
[25] X. Zhang, *Stochastic volterra equations in banach spaces and stochastic partial differential equation*, J. Funct. Anal., *258* (2010),1361–1425.